This ESI for *J. Mater. Chem. A*, 2019, 7, 8559-8567, originally published on 21st March 2019, was updated on 20th May 2019, to fix an error in the legend of Fig. S6(b) ('orthorhombic' has been changed to 'cubic').

Effects of LiBOB on Salt Solubility and BiF_3 Electrode Electrochemical Properties in Fluoride Shuttle Batteries

Asuman Celik Kucuk[a*], Taketoshi Minato[a], Toshiro Yamanaka[a], Takeshi Abe[b*]

Office of Society-Academia Collaboration for Innovation, Kyoto University, Katsura, Nishikyo, Kyoto 615-8530, Japan.
Graduate School of Global Environmental Studies, Kyoto University, Katsura, Nishikyo, Kyoto 615-8530, Japan.

Supporting information

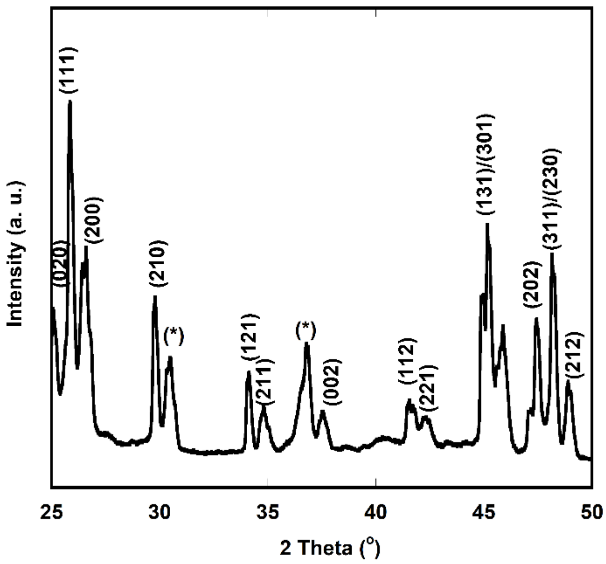

Fig. S1 X-ray diffraction patterns of BiF_3/C in the pristine state; * represents the peak related to the pocket.

Table S1 Reference solutions prepared using tetraglyme (G4) and lithium bis(oxalato)borate (LiBOB)

Code	LiBOB (M)
$LiBOB_{0.06}$/G4	0.06 (1 wt%)
$LiBOB_{0.25}$/G4	0.25 (4.4 wt%)
$LiBOB_{0.5}$/G4	0.5 (9 wt%)

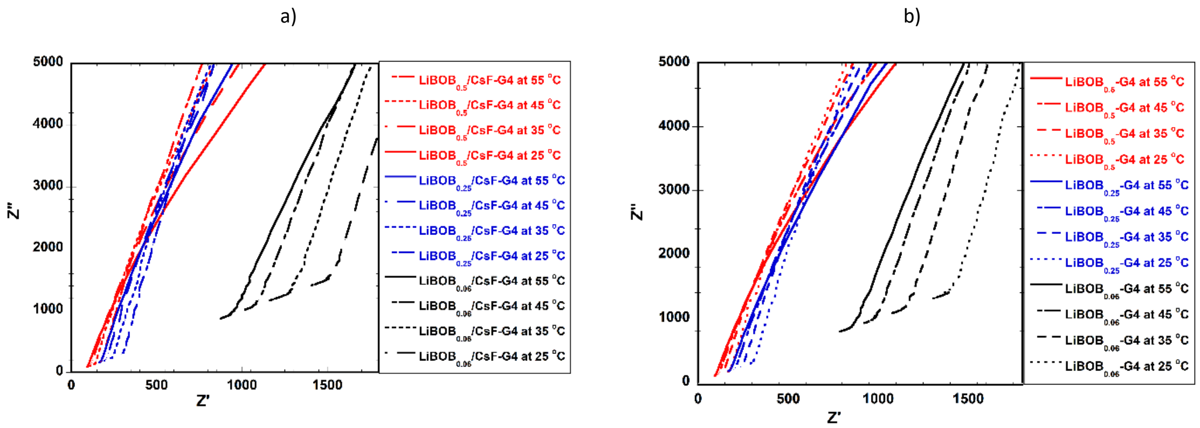

Fig. S2 Temperature and concentration dependence of the ionic conductivity for the (a) $LiBOB_n$/CsF/G4 and (b) $LiBOB_n$/G4 electrolyte solutions (LiBOB: lithium bis(oxalato)borate; G4: tetraglyme; n: LiBOB molar concentration).

Table S2 Comparison between the temperature dependence of the conductivity of the $LiBOB_n$/CsF/G4 and $LiBOB_n$/G4 solutions (LiBOB: lithium bis(oxalato)borate; G4: tetraglyme, Ea; Activation Energy)

	25˚C	35˚C	45˚C	55˚C	Ea (kj/mol)
$LiBOB_{0.06}$/G4	3.98×10^{-4}	4.65×10^{-4}	5.08×10^{-4}	5.87×10^{-4}	15.6
$LiBOB_{0.06}$/CsF/G4	3.64×10^{-4}	4.21×10^{-4}	4.57×10^{-4}	5.37×10^{-4}	16.18
$LiBOB_{0.25}$/G4	1.28×10^{-3}	1.57×10^{-3}	1.88×10^{-3}	2.19×10^{-3}	14.32
$LiBOB_{0.25}$/CsF/G4	1.31×10^{-3}	1.63×10^{-3}	1.95×10^{-3}	2.28×10^{-3}	14.7
$LiBOB_{0.5}$/G4	2.24×10^{-3}	2.81×10^{-3}	3.43×10^{-3}	4.00×10^{-3}	10.21
$LiBOB_{0.5}$/CsF/G4	2.27×10^{-3}	2.86×10^{-3}	3.49×10^{-3}	4.17×10^{-3}	10.15

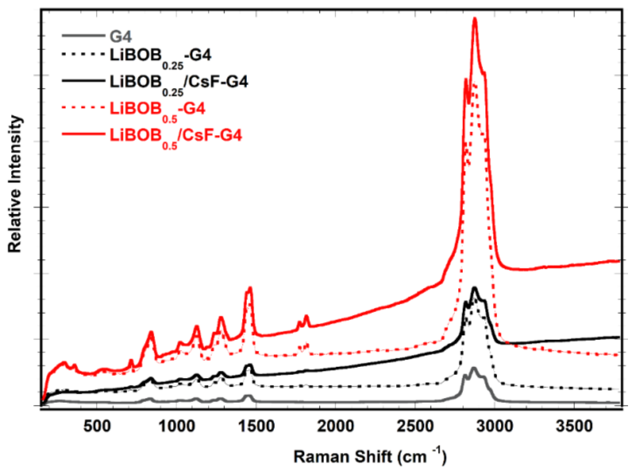

Fig. S3 Raman spectra of $LiBOB_{0.25}$/CsF/G4, $LiBOB_{0.5}$/CsF/G4, $LiBOB_{0.25}$/G4, $LiBOB_{0.5}$/G4, and pure G4 in the of 200–3800 cm^{-1} region (LiBOB: lithium bis(oxalato)borate; G4: tetraglyme).

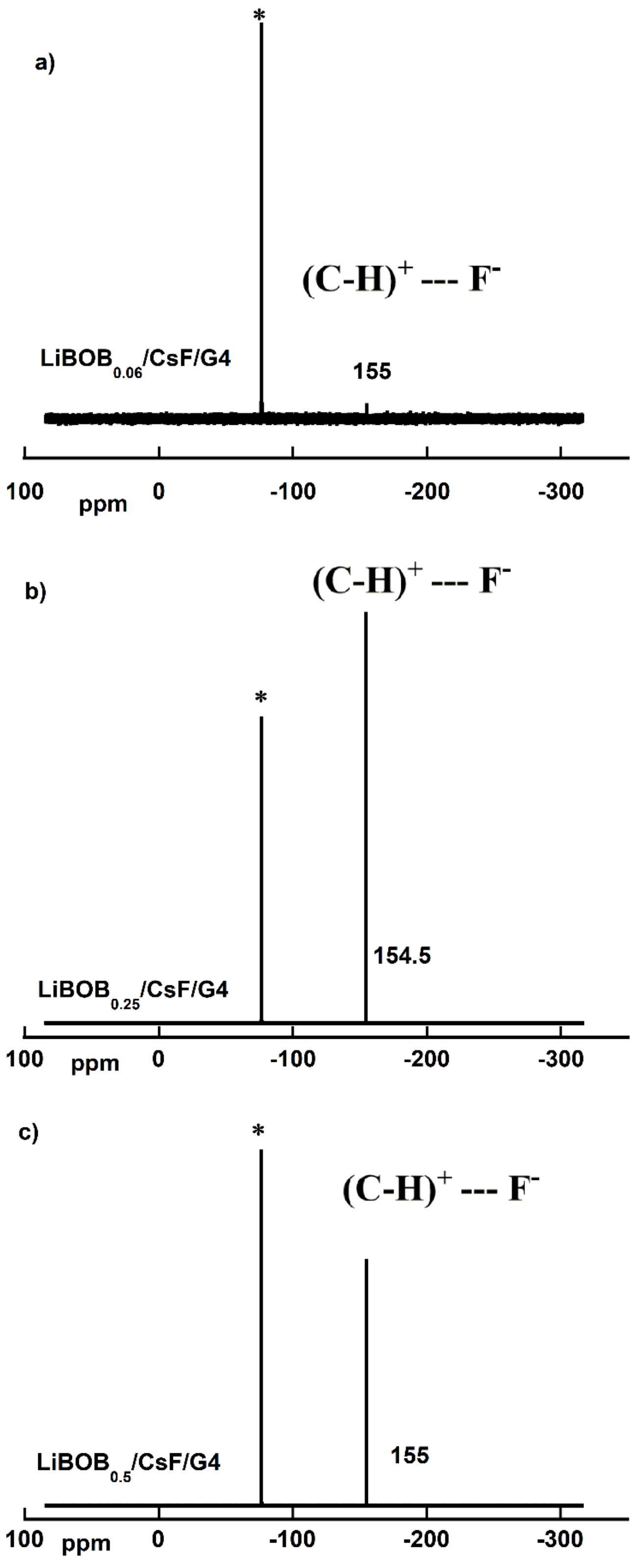

Fig. S4 ^{19}F NMR spectra of (a) $LiBOB_{0.06}/CsF/G4$, (b) $LiBOB_{0.25}/CsF/G4$, and (c) $LiBOB_{0.5}/CsF/G4$ electrolytes. Chemical shift related to the reference of trifluoroacetic anhydride (TFAA) at −76.5 ppm is shown with an asterisk (*).

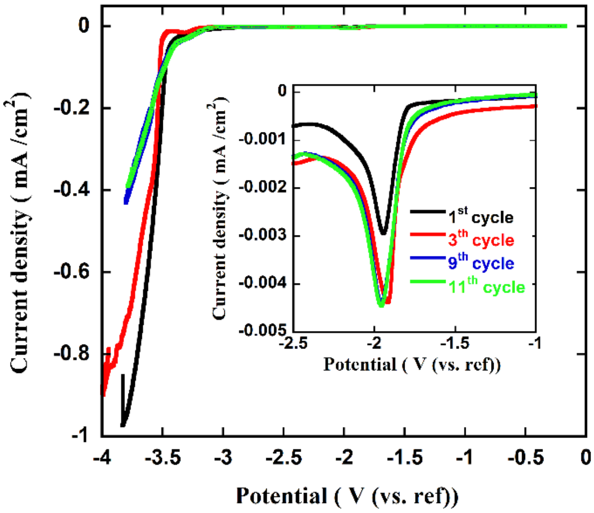

Fig. S5 Linear sweep voltammograms of the glassy carbon electrode in $LiBOB_{0.25}$/CsF/G4 (LiBOB: lithium bis(oxalato)borate; G4: tetraglyme) in the potential range from −4.0 to 0.0 V (vs reference electrode) at a scan rate of 1 mV s^{-1}.

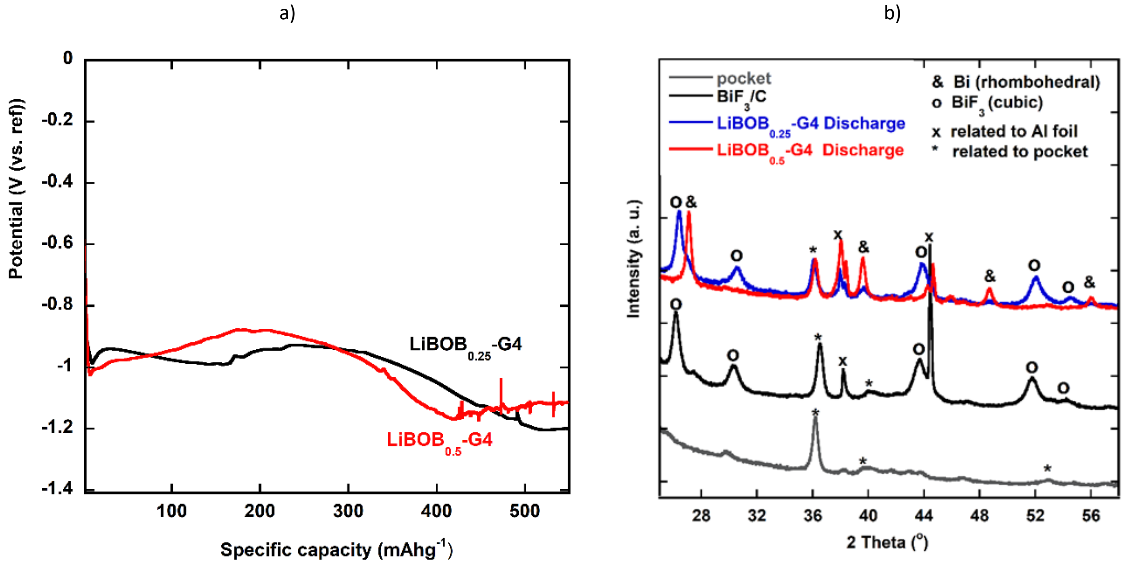

Fig. S6 (a) Initial first discharge–charge curves of the BiF_3/C nanocomposite electrodes, cycled at room temperature and 1/40 C rate in $LiBOB_{0.25}$/G4 and $LiBOB_{0.5}$/G4, containing 0.25 M and 0.5 M LiBOB (discharging cutoff voltage: −1.6 V), respectively. (b) X-ray diffraction patterns of BiF_3/C in the pristine, fully discharged states for $LiBOB_{0.25}$/G4 and $LiBOB_{0.5}$/G4. (LiBOB: lithium bis(oxalato)borate; G4: tetraglyme.)

Table S3 Relation between capacity and cycling number for $LiBOB_{0.25}$/CsF/G4 (LiBOB: lithium bis(oxalato)borate; G4: tetraglyme) at 1/40 C rate

Cycle Number	1st	2nd	3rd	4th	5th	6th
Discharge capacity (mAh g^{-1})	340	116	93	80	72	70
Charge capacity (mAh g^{-1})	117	86	75	70	65	70